



# Purification of saturated $\text{LiNO}_3$ solution using titanium phosphate ion-exchanger: Equilibrium study

V. I. IVANENKO, M. V. MASLOVA, P. E. EVSTROPOVA, L. G. GERASIMOVA

Tananaev Institute of Chemistry and Technology of Federal Research Centre,  
Kola Science Centre of the Russian Academy of Sciences, Apatity, Russia

Received 7 April 2022; accepted 5 July 2022

**Abstract:** Sorption properties of titanium phosphate ion-exchanger (Li-TiOP) towards  $\text{Cu}^{2+}$ ,  $\text{Co}^{2+}$ ,  $\text{Mn}^{2+}$ ,  $\text{Ni}^{2+}$  and  $\text{Cr}^{3+}$  ions in saturated  $\text{LiNO}_3$  solution were investigated. Solid samples were characterized by XRD, SEM, TG, DSC, NGSP and elemental analysis. Concentrations of elements in the solutions were determined by AAS and ICP MS methods. The adsorption isotherms for studied metal ions were calculated using the Langmuir, Freundlich, Temkin and Nikolsky models. Necessity for allowing for the solvated state of the sorbate is shown in studying the sorption of metal ions. Selectivity of Li-TiOP towards studied ions is found to be described in the following order of  $\text{Cr}^{3+} > \text{Cu}^{2+} > \text{Mn}^{2+} > \text{Co}^{2+} > \text{Ni}^{2+}$  for all models. The change in the thermodynamic parameters of the sorption process is associated with that in the ionic potential of the sorbent. Titanium phosphate effectively removes trace concentrations of metal ions from multi-component solutions, resulting in achievement of  $\text{LiNO}_3$  purity level of  $>99.999$  wt.%.

**Key words:** lithium nitrate; titanium phosphate; purification; transition metal elements; sorption; adsorption isotherm; thermodynamics

## 1 Introduction

Among a variety of functional materials, lithium-containing compounds are of a great interest. Due to their unique characteristics, they are widely used in lithium ion batteries (LIBs) [1,2]. Owing to high redox potential and specific heat capacity, LIBs become a key element of modern electric vehicle, cellular phones and laptop computers [3]. Lithium compounds are used in special ceramics with ferro-, pyro-, piezo- and electro-optical properties [4–8].

Brines and high-grade lithium ores are the primary sources of lithium. Lithium recovery from ore or clay consists of mineral processing and concentration followed by the hydro- or pyrometallurgy process [9–11]. For lithium recovery

from brines with various techniques, such as precipitation, solvent extraction, desalination, membrane separation and electrodialysis, can be applied [12–17]. Lithium is industrially produced mainly as lithium carbonate, lithium hydroxide, and lithium chloride. No matter what resources or methods are used, deep purification is always necessary for production of high purity lithium products from  $\text{Li}^+$  concentrated solution with some sodium, potassium, and calcium as the common impurities. Lithium salt of purity grade of more than 98 wt.% can be obtained employing precipitation techniques [18]. Such industrial grades, however, are not applicable on production of LIB, special glass and ceramics, thermal nuclear systems, and optical and biomedicine materials which require lithium carbonate purities of more than 99.5–99.9 wt.% [19]. The presence of undesirable

impurities in Li precursor leads to an uncontrolled change in functional properties of final compounds. Therefore, Li salts of industrial grades to meet higher purity standards require additional processing which involves a number of purification techniques such as precipitation [18,20,21], ion-exchange [22–25], liquid–liquid or solvent extraction [26–30], and membranes [12,15,31]. The attention of researchers is focused on the purification of solutions from alkali and alkaline metals. Although the most harmful impurities for special glass and ceramics are transition metals, these metal ions will enter the lithium solution when they contact with construction materials during processing or in recycling of LIBs. Transition metals contained in the lithium precursor change composition and structure of the ceramic and glass products during heat treatment. In functioning of optical materials for laser-cooling crystal, the transition-metal impurities play a dramatic role reducing the cooling efficiency. For optical materials the concentration of transition metals should not exceed 0.00005, 0.00002, 0.00005, 0.00002, 0.00005 wt.% for Cu, Co, Mn, Ni and Cr, respectively.

Some methods were proposed to eliminate transition metals impurities. The most popular purification method is precipitation. LINNEEN et al [18] developed multistage crystallization process to obtain high-purity  $\text{Li}_2\text{CO}_3$  of 99.95%. The heavy metal cations were isolated as hydroxides, while LiOH was added to the lithium solution. The main disadvantages of this method are an influence of the ionic strength and the concentration of Li in the solution on the solubility of metal hydroxides.

Removal of transition metals from lithium salts ( $\text{Li}_2\text{CO}_3$  and LiCl solutions) was performed by sorption technique using chelating commercial materials such as Purolite S930, Amberlite IRC 748 and AXIONIT 3S [32]. These materials possess a selectivity towards certain transition metals, and combination of the sorbents allows achieving the purification level of 99.90% with residual concentration of 0.0002, 0.001, 0.001, 0.0007 wt.% for Mn, Cr, Ni and Cu ions, respectively.

Another strategy for purifying Li starting material for crystal growth was based on the multistage chelate-assisted solvent extraction (CASE). Ammonium pyrrolidine dithiocarbamate

(APDC) as a chelating agent has a high affinity for complexation of impurity ions. The process started with mixing an aqueous lithium solution and an immiscible organic solvent to form a two-phase system. Metal-chelate complexes have a lower solubility in the aqueous than that in the organic phase, and impurities were concentrated in the organic phase which was removed [33].

HEHLEN et al [34] used ethylenediamine tetraacetic acid (EDTA) as a chelating agent and showed that lithium carbonate  $\text{Li}_2\text{CO}_3$  of high purity can be obtained (99.999%). Lithium nitrate solution in the purification procedure is more effective than lithium carbonate solution due to the higher solubility of lithium nitrate and the weaker complexing ability of nitrate ion towards transition metals. So,  $\text{Li}_2\text{CO}_3$  was first dissolved in nitric acid, and the respective nitrate salt was formed by evaporation. The metal nitrate was then dissolved in water, buffered to the optimum pH  $\sim 4$  for solvent extraction, and pressed through a nylon filter ( $<0.2 \mu\text{m}$  pore size) to remove any macroscopic contaminants. The resulting solution was mixed with CASE prepared from EDTA chelate and methyl-isobutyl-ketone as the organic solvent. The CASE steps were repeated four times to achieve required purity.

It is obvious that the deep purification of lithium salt is largely complicated. It is a long multistep process requiring high reagent consumption, so the new simpler procedures are definitely welcome.

In this work, ion-exchange method has been developed to obtain a high-purity  $\text{LiNO}_3$  saturated solution by employing the specially prepared titanium phosphate inorganic ion-exchanger. In contrast to the methods currently used the new approach presented in this work is more simplified. It markedly reduces the number of the purification stages and obtains lithium solution of required purity by an environmentally friendly technique.

## 2 Experimental

### 2.1 Materials

Solid oxotitanium sulphate with  $\text{TiOSO}_4 \cdot \text{H}_2\text{O}$  formula was used as a titanium precursor, and 10% phosphoric acid was used as a phosphorus-

containing agent for titanium phosphate synthesis. Industrial grade  $\text{Li}_2\text{CO}_3$ , analytical grade  $\text{HNO}_3$ ,  $\text{LiOH}\cdot\text{H}_2\text{O}$ ,  $\text{Co}(\text{NO}_3)_2\cdot 6\text{H}_2\text{O}$ ,  $\text{Mn}(\text{NO}_3)_2\cdot 6\text{H}_2\text{O}$ ,  $\text{Cr}(\text{NO}_3)_3\cdot 9\text{H}_2\text{O}$ ,  $\text{Cu}(\text{NO}_3)_2\cdot 9\text{H}_2\text{O}$  and  $\text{Ni}(\text{NO}_3)_2\cdot 6\text{H}_2\text{O}$  were purchased from Neva-Reaktiv (Russia). Stock solutions were diluted with distilled water to produce required concentrations of the chemicals.

## 2.2 Synthesis of titanium phosphate sorbent (TiOP)

100 g of titanium salt was added to 10%  $\text{H}_3\text{PO}_4$  solution under constant stirring at 60 °C, and the resulting suspension was kept for 5 h. The molar ratios of Ti to P was 1:1. The solid obtained was separated by filtration and washed with  $\text{H}_2\text{O}$  at a solid to liquid ratio of 1:20.

For sorption experiments, the titanium phosphate obtained was treated with 0.2 mol/L  $\text{LiOH}$  to produce the Li-substituted form of titanium phosphate. The route of the synthesis was as follows: to avoid the hydrolysis of TiOP, 100 mL of 0.5 mol/L  $\text{LiNO}_3$  was mixed with 10 g of TiOP, and then 50 mL of 1 mol/L  $\text{LiOH}$  was dropwise added to the mixture under constant stirring at 60 °C. The suspension was kept under stirring for 2 h before filtration. The resulting sorbent (Li-TiOP) was washed with water and dried at 60 °C.

## 2.3 Preparation of saturated $\text{LiNO}_3$ solution

788.6 mL of  $\text{HNO}_3$  with concentration of 799 g/L was mixed with 500 mL of distilled water. 369.4 g of  $\text{Li}_2\text{CO}_3$  was gradually added to the solution, and the final pH of the solution was about 4. Then, 1 mol/L  $\text{LiOH}$  was added to the solution until pH value reached 5–5.5. As a result, 5 mol/L  $\text{LiNO}_3$  solution was obtained.

To produce the contaminated  $\text{LiNO}_3$  solution, corresponding  $\text{Co}(\text{NO}_3)_2$ ,  $\text{Mn}(\text{NO}_3)_2$ ,  $\text{Cr}(\text{NO}_3)_3$ ,  $\text{Cu}(\text{NO}_3)_2$  and  $\text{Ni}(\text{NO}_3)_2$  solutions or their mixture at required concentrations of impurities were added to 5 mol/L  $\text{LiNO}_3$ .

## 2.4 Characterization techniques

Elemental analysis of sorbent obtained was carried out by dissolving the solid in the mixture of  $\text{HF}$ ,  $\text{HNO}_3$  and  $\text{HCl}$ , and the solution was analyzed by direct-current plasma emission spectroscopy using a Shimadzu ICPE-9000 spectrometer. The thermogravimetric (TG/DTG) and differential

scanning calorimetric (DSC) data of sample were collected using a thermogravimetric analyzer (Netzsch STA 409 PC/PG) under argon atmosphere. PXRD data were obtained by Shimadzu D6000 diffractometer with monochrome  $\text{Cu K}\alpha$  radiation ( $\lambda=1.5418 \text{ \AA}$ ). SEM images were obtained by using a scanning electron microscope SEMLEO-420. The surface area of the samples was determined by low-temperature nitrogen adsorption, using a surface analyzer Tristar 320. The pore size distribution was calculated using the BJH method. The concentration of transition metals in the filtrates from all sorption experiments was determined by atomic adsorption by an AAS 300 Perkin-Elmer spectrometer.

## 2.5 Sorption experiments

An experimental study of the purification of saturated  $\text{LiNO}_3$  solution was carried out using the batch technique at 25 °C and pH 5.5. The concentration of transition metals in the  $\text{LiNO}_3$  solution ranged from 0.1 to 4 mmol/L. The sorbent (0.2 g) was mixed with 40 mL solution of certain concentration of metal ions and kept at constant stirring until the equilibrium is attained.

The amount of an adsorbed metal ion was determined by the difference in the concentrations of metal ions in the solution before and after sorption. The sorption amount was calculated as

$$q_e = \frac{C_0 - C_e}{m} \cdot V \quad (1)$$

where  $C_0$  is the initial concentration of the metal ion in the solution,  $C_e$  is the metal ion concentration at equilibrium,  $V$  is the volume of the solution, and  $m$  is the mass of the adsorbent.

For studies of the sorption ability of Li-TiOP depending on solution pH, the initial metal concentration was chosen as 5 mmol/L. The required pH value of the saturated  $\text{LiNO}_3$  solution was adjusted by adding 1 mol/L  $\text{HNO}_3$  or 1 mol/L  $\text{LiOH}$ . 100 mL of the obtained solution and 0.5 g of Li-TiOP were mixed, and the suspension was kept at room temperature under stirring conditions for 24 h. The final pH values were measured after the interaction of the sorbent with the solution of known initial pH. The metal removal by the sorbent was evaluated by its adsorption capacity ( $q_e$ ).

In order to further investigate the properties of Li-substituted TiOP sorbent, an additional sorption experiment was performed. Five different metal salts were mixed in 1 L of saturated NaNO<sub>3</sub> solution (345 g/L). The concentration of metal ions in the solution varied from 0.005 to 0.012 g/L, which corresponded to 0.007–0.017 wt.% of impurities in lithium nitrate. The sorption was carried out under the same conditions at pH 5.5 for 8 h. To estimate the selectivity, the distribution coefficient ( $K_d$ ) of studied ions was calculated as [35]

$$K_d = \frac{C_o - C_e}{C_e} \cdot \frac{V}{m} \quad (2)$$

## 2.6 Sorption equilibrium studies

Both empirical and theoretical isotherm models were used to describe ion exchange equilibrium. To obtain quantitative characteristics of the sorption process, several empirical models were applied using linearized equations of the Langmuir (Eq. (3)), Freundlich (Eq. (4)), and Temkin (Eq. (5)) isotherms [32].

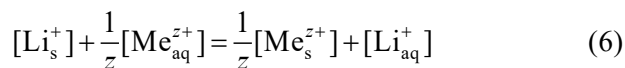
$$\frac{1}{q_e} = \frac{1}{b q_{\max} C_e} + \frac{1}{q_{\max}} \quad (3)$$

$$\ln q_e = \ln K_F + \frac{1}{n} \ln C_e \quad (4)$$

$$q_e = B \ln A_T + B \ln C_e \quad (5)$$

where  $q_e$  is the amount of adsorbate in the adsorbent at equilibrium;  $q_{\max}$  is the maximum of the capacities;  $b$  is the Langmuir isotherm constant related to the intensity of the sorption process;  $K_F$  is the Freundlich isotherm constant related to the adsorption capacity, and  $n$  is the parameter indicating the adsorption intensity and the system heterogeneity;  $A_T$  is the Temkin isotherm equilibrium binding constant;  $B = (RT)/b_T$ , where  $b_T$  corresponds to the difference in enthalpy between the zero and the full coverage;  $R$  is the molar gas constant;  $T$  is the temperature.

Theoretical isotherm model is based on the law of mass action (LMA). In this method, the ion exchange process is considered as a chemical reaction and describes the real behavior of ions in both the solution and sorbent phases [36]. The following expression represents the chemical reaction between metal ions and sorbent particles:



where  $[Li_s^+]$  and  $[Me_s^{z+}]$  are the concentrations of lithium and metal ions in the solid phase, respectively,  $[Me_{aq}^{z+}]$  and  $[Li_{aq}^+]$  are the corresponding ion concentrations in the liquid phase, and  $z$  is the charge of metal ions.

Applying mass balance approach to the solid and liquid phases gives the following isotherm equation (Nikolsky isotherm):

$$\frac{[Me_s^{z+}]}{[Me_{aq}^{z+}]^{1/z}} = K_N \frac{[Li_s^+]}{[Li_{aq}^+]} \quad (7)$$

Linearized equations of Nikolsky model can be represented as follows:

$$\left( \frac{q_e}{C_e} \right)^{1/z} = \left[ \frac{K_N}{[Li_{aq}^+](1/(1/z))^{1/z}} \right] q_{\max} - \left[ \frac{K_N}{[Li_{aq}^+](1/(1/z))^{1/z}} \right] q_e \quad (8)$$

where  $K_N$  is the Nikolsky isotherm constant. This equation makes it possible to determine the stoichiometry of a heterogeneous sorption process with equivalent substitution of some ions for others.

## 3 Results and discussion

### 3.1 Characterization of sorbent

Elemental analysis data for the as-synthesized titanium phosphate give a composition of 22.8 at.% Ti and 15.3 at.% P, which corresponds to a Ti to P molar ratio of 1:1.

According to the XRD data, the products obtained are amorphous. The calcination at 750 °C results in the formation of a phase with the composition of Ti<sub>2</sub>O(PO<sub>4</sub>)<sub>2</sub> (Fig. 1).

According to the thermogravimetric curve of initial titanium phosphate (Fig. 2), mass losses of 10.86% and 8.69% are observed at 25–180 °C and 180–650 °C, respectively. A broad endothermic peak at 120.9 °C occurs due to the removal of adsorbed and coordinated water molecules. Within the temperature of 180–650 °C two concurrent processes take place: the condensation of hydroxo- and hydrogen-phosphate groups. Above 650 °C the mass loss is 0.42%. The total mass loss is 19.77% that corresponds to five water molecules.

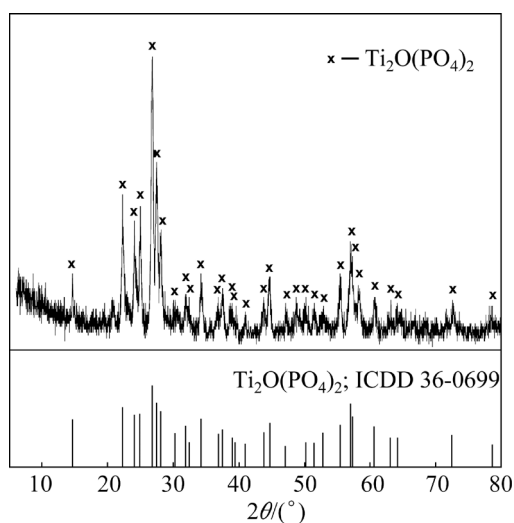


Fig. 1 XRD pattern of initial product calcined at 750 °C

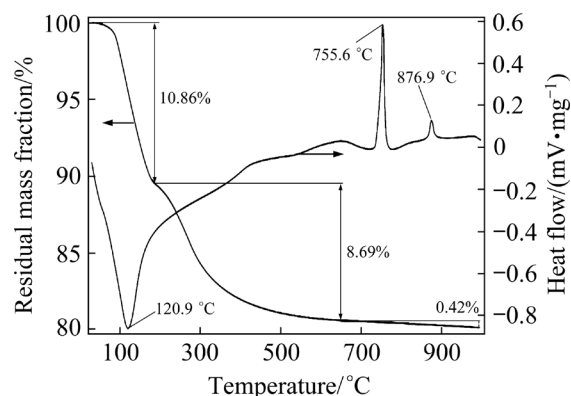
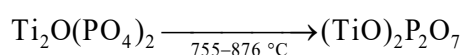
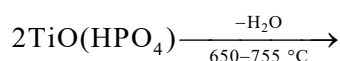
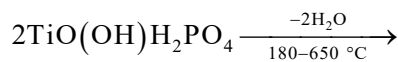
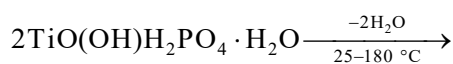


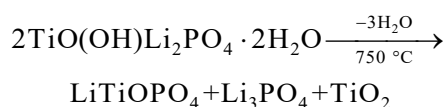
Fig. 2 TG-DSC curves for TiOP product obtained

Exothermic peaks at 755.6 and 876.9 °C are observed which correspond to the titanium phosphates transformation into the  $\text{Ti}_2\text{O}(\text{PO}_4)_2$  and  $(\text{TiO})_2\text{P}_2\text{O}_7$  phases, respectively, according to the thermolysis process:



For Li-substituted titanium phosphate the final composition can be represented as follows: 21.2% Ti, 13.7% P, 6.13% Li. The  $\text{Li}^+$  uptake is calculated to be 8.82 mmol/g which is in good agreement with the IEC calculated from the  $\text{TiO}(\text{OH})\text{Li}_2\text{PO}_4 \cdot 2\text{H}_2\text{O}$  formula (8.85 mmol/g).

The Li-substituted titanium phosphate is also amorphous in nature. This material is thermally unstable and the calcination at 750 °C results in the formation of mixture of phases with the composition of  $\text{LiTiO}(\text{PO}_4)$ ,  $\text{Li}_3\text{PO}_4$ , and  $\text{TiO}_2$  (Fig. 3) according to the scheme as



According to the TG–DSC curves (Fig. 4), the mass loss of 12.26% is observed at 25–250 °C due to the loss of adsorbed and coordinated water molecules, and no notable mass loss is found with further increase in temperature. At temperature above 300 °C decomposition of the sorbent occurs. Three exothermic peaks detected at 307, 406 and 604 °C correspond to the transformation of  $\text{TiO}(\text{OH})\text{Li}_2\text{PO}_4 \cdot 2\text{H}_2\text{O}$  into  $\text{Li}_3\text{PO}_4$ ,  $\text{LiTiO}(\text{PO}_4)$ , and  $\text{TiO}_2$  (anatase) [37,38].

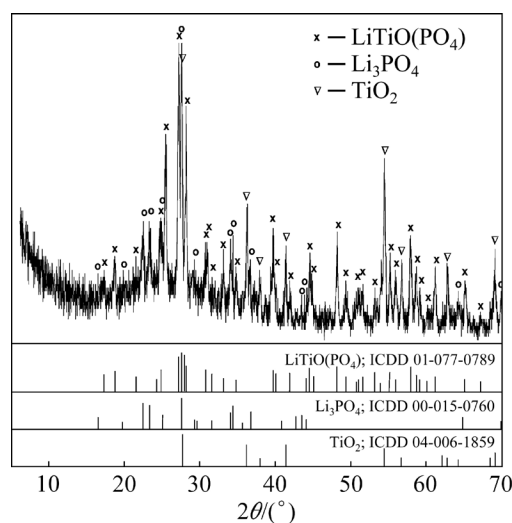


Fig. 3 XRD pattern of Li-TiOP product calcined at 750 °C

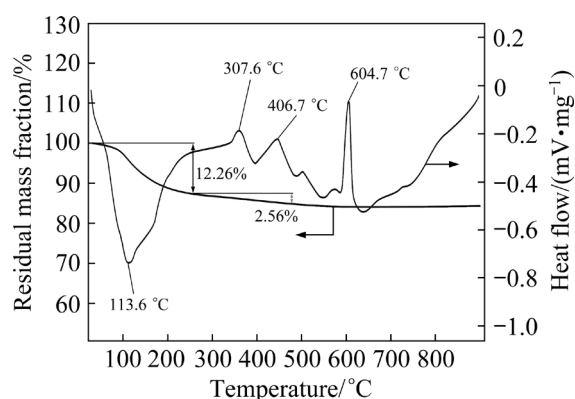


Fig. 4 TG–DSC curves for Li-TiOP product

The porous structure of the sorbent largely affects the availability of exchange groups, and consequently, the functional properties of the material. The measured textural properties of the initial (TiOP) and Li-substituted (Li-TiOP) products allow us to characterize the materials obtained as a mesoporous material (Table 1).

**Table 1** Textural properties of sorbent

Sorbent	Surface area/ ( $\text{m}^2 \cdot \text{g}^{-1}$ )	Total pore volume/ ( $\text{cm}^3 \cdot \text{g}^{-1}$ )	Average pore diameter/ nm
TiOP	141.7	0.431	9.63
Li-TiOP	33.1	0.075	8.55

It can be seen that replacing hydrogen ions by lithium ones in the sorbent leads to pronounced decrease in the specific surface area and total pore volume that may be related to the increase in orderliness of the matrix of the final material.

The morphological features of the material obtained are shown in Fig. 5. The solid shows a morphology of relatively small agglomerates with average size of 6–8  $\mu\text{m}$  formed by “flake” particles with size of 300–600 nm oriented in one direction.

### 3.2 Effect of solution pH on uptake of metal ions by Li-TiOP

The effect of solution pH on the metal ions uptake by Li-TiOP was tested, and the results are presented in Fig. 6. The selected range of pH values corresponding to the metal species in solutions was as follows: 2–5 for  $\text{Cu}^{2+}$  and  $\text{Cr}^{3+}$ , 2–7.5 for  $\text{Co}^{2+}$  and  $\text{Ni}^{2+}$ , and 2–8 for  $\text{Mn}^{2+}$ . The removal efficiency of studied metal ions increases with the increase of solution pH, and is associated with the ion-exchange process.

The ion-exchange sorption on the titanium phosphates is caused by the increased mobility of the lithium ions of the functional phosphate groups, which are polarized in the internal coordination sphere of Ti(IV). This phenomenon makes the exchange of the lithium on metal cations possible. The equivalent amount of lithium ions is released into the solution from the lithium-substituted form of titanium phosphate, and the equivalent amount of chromium, copper, manganese, nickel and cobalt cations is adsorbed by the titanium phosphate.

The functional groups of cation-exchangers are known to be active when they are deprotonated.

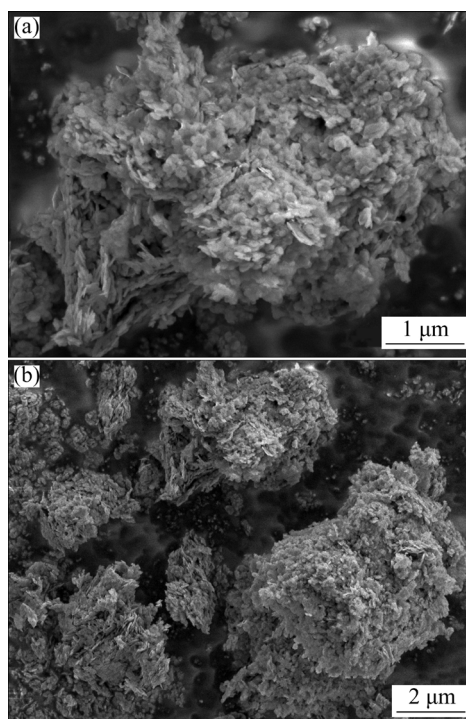


**Fig. 5** SEM images of Li-TiOP synthesized

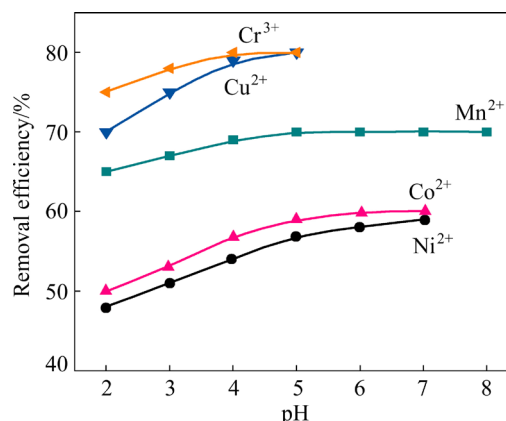


**Fig. 6** Effect of solution pH on transition metal ions sorption onto Li-TiOP (The initial concentration of transition metals is 5 mmol/L, and contact time is 24 h)

The dissociation constants of the functional groups of titanium phosphate  $\text{TiO}(\text{OH})\text{H}_2\text{PO}_4 \cdot 2\text{H}_2\text{O}$ ,  $\text{p}K_1$  and  $\text{p}K_2$  (2.2 and 7.1, respectively) are close to  $\text{p}K$  of  $\text{H}_3\text{PO}_4$  [39]. Therefore, at pH around 2.2, about half of the exchangeable ions of the first  $\text{H}_2\text{PO}_4^-$  species of the adsorbent are involved in the ion exchange process. The rest can be released under neutral and alkaline conditions. The theoretical ion-exchange capacity of Li-TiOP is 8.85 mmol/g. So, at pH ~2, the theoretical sorption capacity is expected to be 2.2 mmol/g. The results demonstrate that at the abovementioned pH, the sorption

capacities of  $\text{Cr}^{3+}$ ,  $\text{Cu}^{2+}$ ,  $\text{Mn}^{2+}$ ,  $\text{Co}^{2+}$  and  $\text{Ni}^{2+}$  ions are 2.1, 1.5, 1.3, 1.0 and 0.96 mmol/g, respectively. The sorption efficiency of Li-TiOP towards all studied ions at pH 2 in the electrolyte solution exceeds 50%. It can be due to a considerably lower amount of solute compared to the quantity of active sorption sites capable of exchanging, so the sorption process occurs without any hindrance. Low sorption efficiency of Li-TiOP towards cobalt and nickel ions is associated with the process of the dehydration of the adsorbed ions.

### 3.3 Sorption equilibrium

The sorption capacity of Li-TiOP was evaluated by considering the obtained sorption isotherms. It can be seen from Fig. 7 that material possesses quite high sorption capacity for the tested cations even in highly concentrated (5 mol/L) electrolyte solutions. The type of Cu and Cr isotherms is called “high affinity isotherm”. So, Cu and Cr ions possess great affinity to lithium phosphate compared with other studied ions.

According to the curves obtained in chosen concentration range, the maximum of sorption capacity is not achieved. Additional sorption experiments were performed and found that the maximum values of static ion-exchange capacity at 298 K are as follows (mmol/g): 1.08 for  $\text{Co}^{2+}$ , 1.16 for  $\text{Ni}^{2+}$ , 1.53 for  $\text{Mn}^{2+}$ , 1.80 for  $\text{Cu}^{2+}$  and 1.32 for  $\text{Cr}^{3+}$ . The sorption capacity of sorbent increases slightly with increase in temperature. Our previous results show that the sorption capacities (mmol/g) of TiOP in aqua solution are 1.12–1.60, 1.40, 1.50 and 1.45 for  $\text{Co}^{2+}$ ,  $\text{Ni}^{2+}$ ,  $\text{Cu}^{2+}$  and  $\text{Mn}^{2+}$  ions,

respectively [35,37]. The sorption capacities of titanium phosphates with different compositions are found to be 0.48–1.9, 0.46–0.56, 0.08–0.12, 0.33 and 0.22 mmol/g for  $\text{Cu}^{2+}$ ,  $\text{Co}^{2+}$ ,  $\text{Ni}^{2+}$ ,  $\text{Mn}^{2+}$  and  $\text{Cr}^{3+}$  ions, respectively [40–44]. The values of the metal uptake on TiOP and Li-TiOP are among the highest values reported for different TiP.

The experimental data obtained from the isotherms are interpreted according to the selected adsorption models by plotting  $1/q_e$  vs  $1/C_e$  for the Langmuir model (Fig. 8),  $\ln q_e$  vs  $\ln C_e$  for the Freundlich model (Fig. 9),  $q_e$  vs  $\ln C_e$  for the Temkin model (Fig. 10), and  $(q_e/C_e)^{1/2}$  vs  $q_e$  for the Nikolsky model (Fig. 11). The parameters of the adsorption models are presented in Tables 2 and 3. The applicability of each model was estimated by the determination coefficient ( $R^2$ ).

Among the four models, the Temkin simulation gave the least satisfactory results compared with the experimental data. For the Langmuir and Nikolsky models, the correlation factor  $R^2$  is high ( $R^2=0.997$ – $0.999$  in Tables 2 and 3). YU et al [45] studied the purification of silver nitrate solution, and also found that adsorption of trace cations on the ion-exchange resin D301 corresponds to the Langmuir model. Selectivity of Li-TiOP towards studied ions is found to be in the following order:  $\text{Cr}^{3+} > \text{Cu}^{2+} > \text{Mn}^{2+} > \text{Co}^{2+} > \text{Ni}^{2+}$  for all selected models. This order is in a good agreement with the product solubility constants of metal phosphate species. Chromium phosphate is insoluble compound, and other metal phosphates have the following solubility values: CuP  $1.4 \times 10^{-37}$ , MnP  $7.9 \times 10^{-35}$ , CoP  $2.1 \times 10^{-35}$ , NiP  $4.74 \times 10^{-32}$  [46].

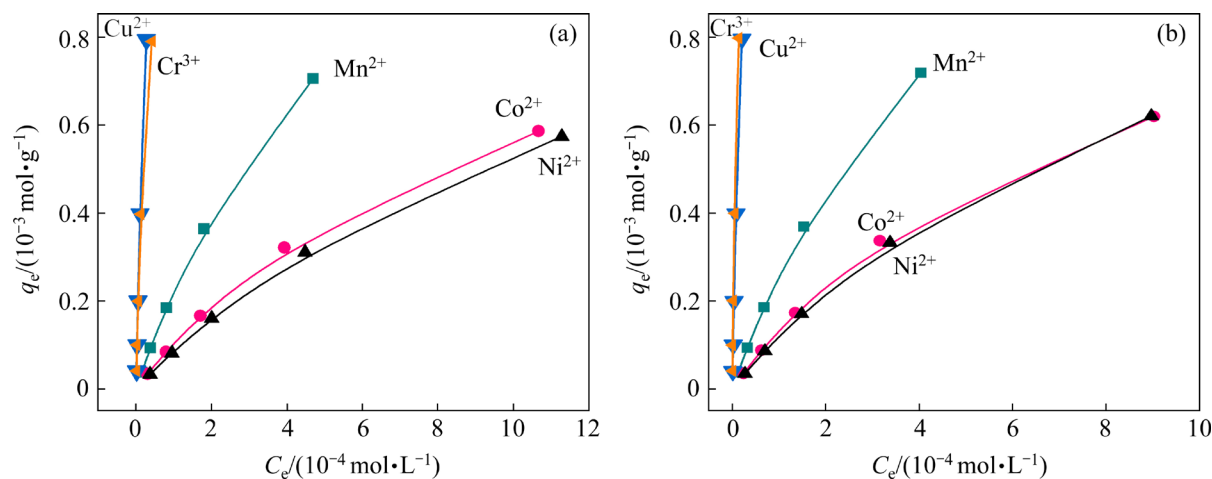


**Fig. 7** Sorption isotherms of  $\text{Mn}^{2+}$ ,  $\text{Co}^{2+}$ ,  $\text{Ni}^{2+}$ ,  $\text{Cu}^{2+}$  and  $\text{Cr}^{3+}$  ions on Li-TiOP at different temperatures: (a) 298 K; (b) 313 K

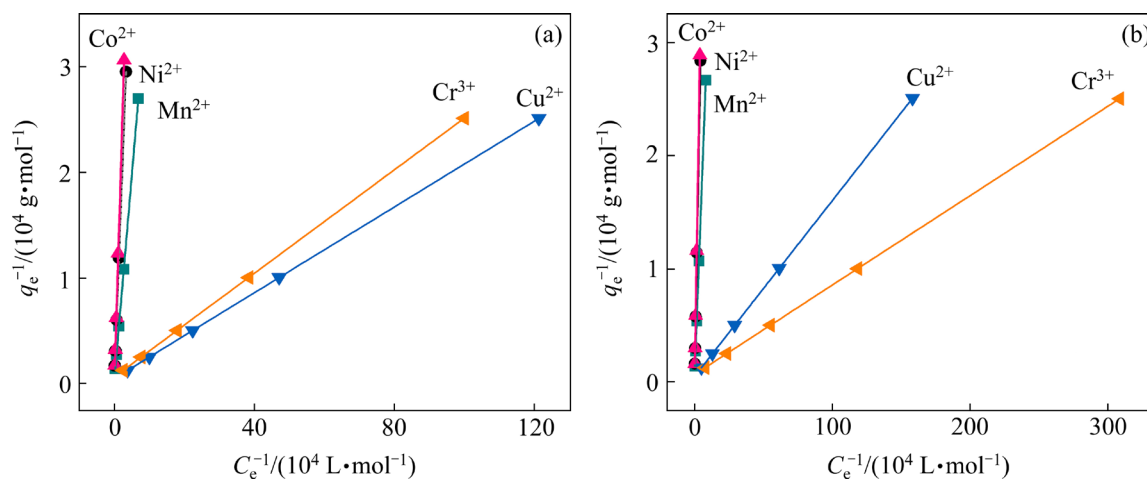


**Fig. 8** Langmuir modeling of experimental sorption data of  $\text{Mn}^{2+}$ ,  $\text{Co}^{2+}$ ,  $\text{Ni}^{2+}$ ,  $\text{Cu}^{2+}$  and  $\text{Cr}^{3+}$  ions on Li-TiOP at 298 K (a) and 313 K (b)

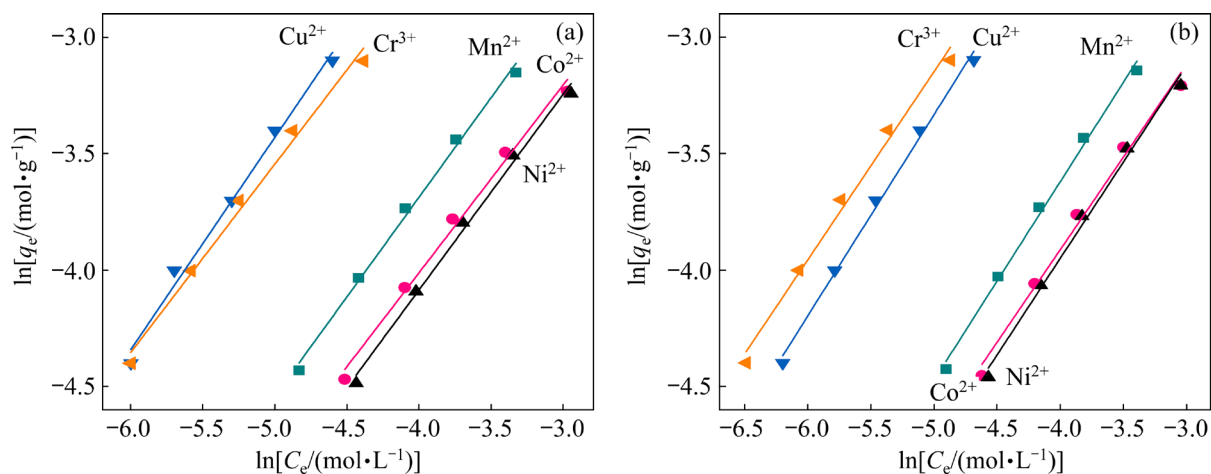


**Fig. 9** Freundlich modeling of experimental sorption data of  $\text{Mn}^{2+}$ ,  $\text{Co}^{2+}$ ,  $\text{Ni}^{2+}$ ,  $\text{Cu}^{2+}$  and  $\text{Cr}^{3+}$  ions on Li-TiOP at 298 K (a) and 313 K (b)

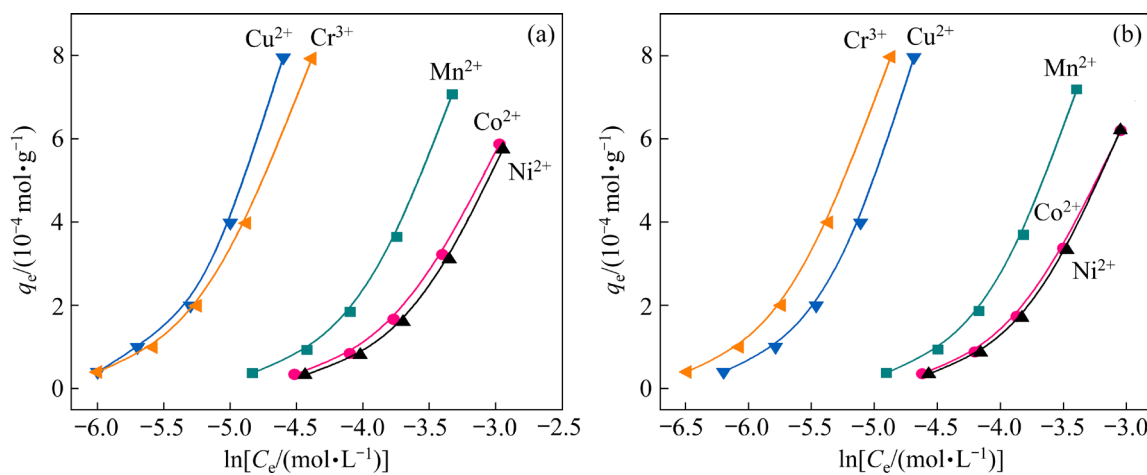


**Fig. 10** Temkin modeling of experimental sorption data of  $\text{Mn}^{2+}$ ,  $\text{Co}^{2+}$ ,  $\text{Ni}^{2+}$ ,  $\text{Cu}^{2+}$  and  $\text{Cr}^{3+}$  ions on Li-TiOP at 298 K (a) and 313 K (b)

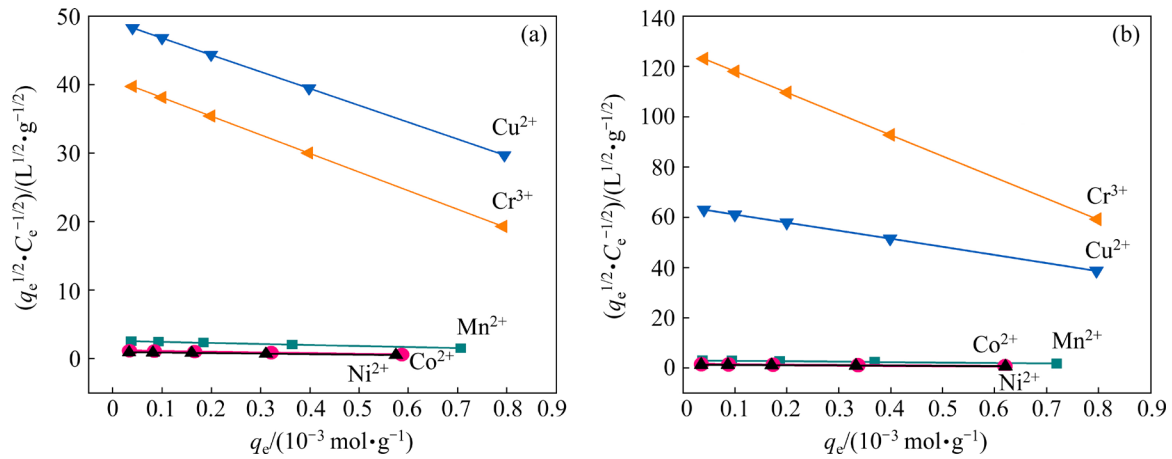


**Fig. 11** Nikolsky modeling of experimental sorption data of  $\text{Mn}^{2+}$ ,  $\text{Co}^{2+}$ ,  $\text{Ni}^{2+}$ ,  $\text{Cu}^{2+}$  and  $\text{Cr}^{3+}$  ions on Li-TiOP at 298 K (a) and 313 K (b)

**Table 2** Parameters for Langmuir and Freundlich isotherm models

Me ion	$T/\text{K}$	$q_{\text{exp}} / (10^{-3} \text{ mol} \cdot g^{-1})$	Langmuir			Freundlich		
			$q_{\text{max}} / (10^{-3} \text{ mol} \cdot g^{-1})$	$b / (10^3 \text{ L} \cdot \text{mol}^{-1})$	$R^2$	$K_F / (10^{-3} \text{ L}^{1/n} \cdot \text{mol}^{1-1/n} \cdot g^{-1})$	$n$	$R^2$
$\text{Mn}^{2+}$	298	0.71	1.61	1.52	0.999	0.77	1.17	0.993
	313	0.72	1.68	1.82	0.999	0.81	1.18	0.993
$\text{Co}^{2+}$	298	0.58	1.13	1.01	0.999	0.46	1.24	0.989
	313	0.62	1.15	1.53	0.999	0.48	1.26	0.986
$\text{Ni}^{2+}$	298	0.57	1.17	0.71	0.999	0.48	1.19	0.992
	313	0.62	1.19	1.02	0.999	0.52	1.21	0.991
$\text{Cu}^{2+}$	298	0.79	1.86	24.64	0.999	2.46	1.10	0.988
	313	0.80	1.90	32.14	0.999	3.11	1.24	0.988
$\text{Cr}^{3+}$	298	0.79	1.37	27.22	0.999	3.20	1.16	0.989
	313	0.80	1.40	37.43	0.999	3.84	1.23	0.994

**Table 3** Parameters for Temkin and Nikolsky isotherm models

Me ion	$T/\text{K}$	$q_{\text{exp}} / (10^{-3} \text{ mol} \cdot g^{-1})$	Temkin			Nikolsky		
			$A_T / (\text{L} \cdot \text{mol}^{-1})$	$b_T / [10^3 (\text{J} \cdot \text{mol}^{-1}) (\text{mol} \cdot \text{kg}^{-1})^{-1}]$	$R^2$	$q_{\text{max}} / (10^{-3} \text{ mol} \cdot g^{-1})$	$K_N / (10^3 \text{ g}^{1/2} \cdot \text{L}^{-1/2})$	$R^2$
$\text{Mn}^{2+}$	298	0.71	6.15	1.75	0.862	1.57	2.69	0.998
	313	0.72	6.18	1.78	0.862	1.59	2.96	0.999
$\text{Co}^{2+}$	298	0.58	6.39	1.59	0.889	1.10	2.14	0.997
	313	0.62	6.45	1.70	0.894	1.12	2.30	0.997
$\text{Ni}^{2+}$	298	0.57	6.37	1.38	0.874	1.16	2.12	0.998
	313	0.62	6.42	1.42	0.879	1.19	2.29	0.998
$\text{Cu}^{2+}$	298	0.79	5.78	1.92	0.856	1.84	9.95	0.999
	313	0.80	5.81	2.03	0.854	1.90	11.49	0.999
$\text{Cr}^{3+}$	298	0.79	5.90	2.15	0.879	1.32	12.77	0.997
	313	0.80	5.92	2.17	0.880	1.32	22.50	0.997

Nikolsky model has demonstrated the best agreement with experimental data. So, Cr(III) ions can be concluded to be adsorbed on lithium-substituted titanium phosphate as a double charged  $\text{Cr}(\text{OH})^{2+}$  ion. This is in a good agreement with the pH change of the solution containing  $\text{Cr}^{3+}$  ions. It has been found that the pH of the solutions of  $\text{Mn}^{2+}$ ,  $\text{Co}^{2+}$ , and  $\text{Ni}^{2+}$  ions does not change during the sorption process. At the same time the pH value of the solution of  $\text{Cu}^{2+}$  and  $\text{Cr}^{3+}$  ions changes markedly. The pH value of the lithium nitrate solution promotes the formation of  $\text{Cr}^{3+}$  hydroxy species. A decrease in the effective charge of the resulting cationic forms of  $\text{Cr}^{3+}$  leads to a weakening of their interaction with the ions present in the solution and a decrease in the size of solvate shell of  $\text{Cr}^{3+}$  ions. As a result, the mobility of  $\text{Cr}^{3+}$  ions increases.  $\text{Cu}^{2+}$  ions are hydrolyzed under chosen experimental conditions to a lesser extent. And the dominant form of ions present in the solution is not the single charged  $\text{Cu}(\text{OH})^+$ , but the aquatic ions of  $\text{Cu}^{2+}_{\text{aq}}$ .

The ion-exchange behaviors of studied ions are also in a good accordance with the solubility product constants of their hydroxy species with the following values:  $\text{Cr}(\text{OH})^{2+}$   $1.26 \times 10^{10}$ ,  $\text{Cu}(\text{OH})^+$   $1 \times 10^7$ ,  $\text{Mn}(\text{OH})^+$   $7.94 \times 10^3$ ,  $\text{Co}(\text{OH})^+$   $2.51 \times 10^4$ , and  $\text{Ni}(\text{OH})^+$   $9.35 \times 10^4$  [47]. Nitrate ions which present at the solutions possess low complexing ability and can form labile outer-sphere complex with metal species. So, they are unlikely to have a significant effect on sorption process.

The sorption of all ions also complies with the Freundlich model ( $R^2 > 0.99$ ). The value of the constant  $1/n$  in the Freundlich equation is less than 1, which indicates the mutual repulsion of adsorbed particles, and consequently, a decrease in the bond energy between the sorbent and sorbate as the surface becomes filled (Table 2). The values of  $K_F$  and  $n$  parameters increase slightly with the increase in temperature. The plot of the Temkin model equation does not give a linear relationship, indicating that the sorption is unlikely to follow this model. For all models, an increase in the maximum sorption capacity of metal cations with the increase of temperature is observed. It may indicate the dehydration of the sorbate and a decrease in the radius of the sorbed ion. The difference in sorption efficiency depends on the size of the effective radius of hydrated ions taking part in the sorption process. This regularity is observed for manganese,

cobalt, and nickel ions. The value of the ionic radii of metal ions increases in the order as follows:  $\text{Ni}^{2+} < \text{Co}^{2+} < \text{Mn}^{2+}$ . So, it is expected that the size of the hydration shell of these metal ions will change in the opposite order, i.e., hydrated ions  $\text{Co}^{2+}$  and  $\text{Ni}^{2+}$  will have a larger radius than  $\text{Mn}^{2+}$  ions. However, no such correlation is found for copper and chromium ions. To gain insight into some mechanisms of interactions between the sorbent and sorbate, the radius and dehydration degree of the adsorbed ions were calculated. We believe that the results are likely to be most correct if ions of the same charge will be compared.

To calculate the size of the hydration shell, we calculated the size of the available site of the solid ( $S$ ) and the effective radius of a sorbed ion ( $r_s$ ). When calculating  $S$ , it is assumed that the entire surface of the sorbent is equally available to the ions of adsorbed metals.

$$S = \frac{S_{\text{BET}}}{q_{\text{max}} N_a} \quad (9)$$

where  $S_{\text{BET}}$  is the specific surface area of the sorbent  $33.14 \text{ m}^2/\text{g}$ ;  $q_{\text{max}}$  is the maximum sorption capacity for the selected cation;  $N_a$  is the Avogadro's number.

The radius of adsorbed ion was evaluated based on the following assumptions:

$$S = (2r_s)^2 = 4r_s^2 \quad (10)$$

hence,

$$r_s = \frac{1}{2} \sqrt{S} \quad (11)$$

The calculated value of effective radius ( $r_s$ ) of adsorbed lithium ion ( $0.394 \text{ \AA}$ ) is less than that of the ionic radius  $r_{\text{cr}}$  ( $0.68 \text{ \AA}$ ) according to Ref. [48]. This discrepancy may be due to the fact that replacing the protons of the phosphate groups of TiOP by lithium ions enhances the titanium phosphate structuring which is confirmed by decrease in the specific surface from 140 to  $33.14 \text{ m}^2/\text{g}$ .

The comparison of ion radii shows that for manganese and copper the values of the adsorbed and ionic radii are close (Table 4).

Obviously, the radii of the sorbed ions of manganese and copper are close. This allows us to infer that the sorption of  $\text{Cu}^{2+}$  and  $\text{Mn}^{2+}$  ions is accompanied by their almost total dehydration. The

**Table 4** Characteristics of non-hydrated and sorbed metal ions at 298 K

Ion	$r_{cr}/\text{Å}$	$r_s/\text{Å}$	$r_s/r_{cr}$	Degree of dehydration, $\alpha/\%$
Mn <sup>2+</sup>	0.91	1.055	1.16	0.17
Co <sup>2+</sup>	0.78	1.40	1.79	1.75
Ni <sup>2+</sup>	0.74	1.51	2.04	2.47
Cu <sup>2+</sup>	0.80	1.06	1.32	0.19

degree of hydration of cobalt and nickel ions increases with a decrease in the ionic radius. This is also confirmed by the comparison between the volumes of the hydrated shell and the non-hydrated ion.

The volume of the hydration shell of the ion in the solution and that of the non-hydrated ion correspond to the following equations:

$$V_{cr} = \frac{4}{3}\pi r_{cr}^3 \quad (12)$$

$$V_s = \frac{4}{3}\pi r_s^3 \quad (13)$$

The volume of the dehydrated shell ( $V_{hydr}$ ) of the adsorbed ion corresponds to

$$V_{hydr} = V_s - V_{cr} = \frac{4}{3}\pi r_s^3 - \frac{4}{3}\pi r_{cr}^3 = \frac{4}{3}\pi(r_s^3 - r_{cr}^3) \quad (14)$$

Hence, the degree of dehydration is as follows:

$$\alpha = \frac{V_{hydr}}{V_{cr}} \quad (15)$$

The degree of hydration of the adsorbed Cr<sup>3+</sup> ions is difficult to estimate as their hydrolysis proceeds and the effective charge of the adsorbed Cr(OH)<sup>2+</sup> decreases. However, it is obvious that both a decrease in the effective charge and an increase in the size of this ion promote a decrease in the hydration degree.

The effective potential of less hydrated ions increases with an increase in the ionic radius and a corresponding decrease in the size of the hydrated shell. Thus, the interaction of adsorbed metal cations with functional groups of the sorbent increases, also the polarization effect increases, enhancing the strength of the interaction. As a result, the sorption of metal cations leads to a decrease in the surface charge due to substitution of hardly polarizable lithium ions by metal ions. The change in the entropy and enthalpy of the sorption process

is suggested to correlate with the change in the ionic potential of the sorbent.

To confirm this assumption, thermodynamic parameters such as enthalpy ( $\Delta H^\ominus$ ), entropy ( $\Delta S^\ominus$ ), and Gibbs free energy change ( $\Delta G^\ominus$ ) for the Langmuir and Nikolsky models were calculated.

$\Delta G^\ominus$  of the sorption process is determined by

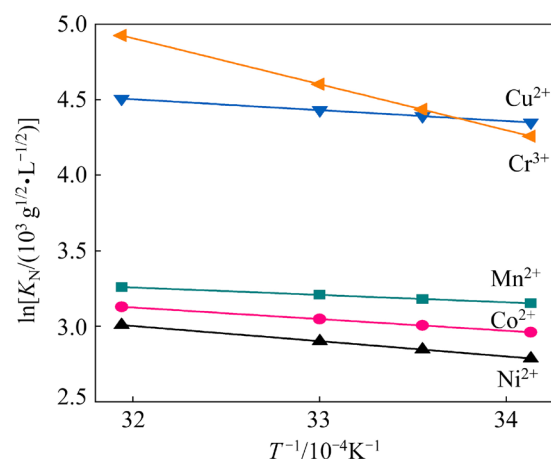
$$\Delta G^\ominus = -2.3RT \cdot \lg K \quad (16)$$

where  $K$  is the Langmuir or Nikolsky isotherm constant.

The standard values of the enthalpy and entropy change are calculated according to the following equation:

$$\lg K = \frac{\Delta S^\ominus}{2.3R} - \frac{\Delta H^\ominus}{2.3RT} \quad (17)$$

The interpretation of the plot of  $\ln K_N$  versus  $1/T$  is carried out using Eq. (17) (see Fig. 12). The values of  $\Delta H^\ominus$  and  $\Delta S^\ominus$  are determined from the slope and intersection of the plot (see Table 5).

**Fig. 12** Plot of  $\ln K_N$  versus  $1/T$ **Table 5** Thermodynamic parameters of sorption process on titanium phosphate

Ion	$\Delta S^\ominus/$ (J·mol <sup>-1</sup> ·K <sup>-1</sup> )	$\Delta H^\ominus/$ (kJ·mol <sup>-1</sup> )	$R^2$	$\Delta G^\ominus_{av}/$ (kJ·mol <sup>-1</sup> )
Mn <sup>2+</sup>	169.52	9.72	0.997	-40.80
Co <sup>2+</sup>	191.26	15.98	0.999	-41.02
Ni <sup>2+</sup>	202.16	20.63	0.998	-39.61
Cu <sup>2+</sup>	207.07	14.45	0.999	-47.26
Cr <sup>3+</sup>	359.27	58.58	0.997	-48.48

The characteristics of the sorption process calculated from the experimental data favour its endothermic nature, and the change in the free energy indicates that there is a specific interaction

between the sorbate and sorbent. The values of  $\Delta H^\ominus$  and  $\Delta S^\ominus$  of the sorption process increase in the order as follows:  $\text{Mn}^{2+} < \text{Co}^{2+} < \text{Ni}^{2+} < \text{Cu}^{2+} < \text{Cr}^{3+}$ . The increase in entropy is so great that it determines the change in the free energy of the process. The change in the thermodynamic characteristics ( $\Delta S^\ominus$  and  $\Delta H^\ominus$ ) of sorption lines up with that in the ionic potential of the adsorbed metal ions (Fig. 13).

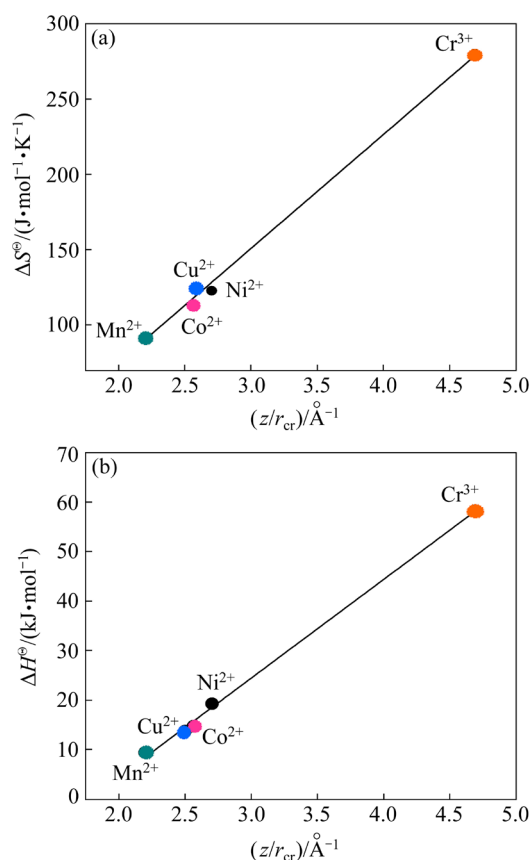


**Fig. 13** Plots of  $\Delta S^\ominus$  (a) and  $\Delta H^\ominus$  (b) vs  $z/r_{cr}$

The positive values of  $\Delta H^\ominus$  and  $\Delta S^\ominus$  indicate the endothermic nature and increased disorderliness of the system, respectively. The increase observed in the entropy change can be caused by both partial dehydration of the sorbate ions and the sorbent surface.

To get insight into the sorption capacity of  $\text{Mn}^{2+}$ ,  $\text{Co}^{2+}$ ,  $\text{Ni}^{2+}$ ,  $\text{Cu}^{2+}$ , and  $\text{Cr}^{3+}$  ions, several points have to be taken into account. These are influence of their ionic radius and ionic potential on adsorption ability and effect the electronic structure of these ions on the interaction with functional groups of the Li-TiOP sorbent.

Metal ions in solution interact with ligands forming bonds with them. In our case, this interaction with aqua ligands are preferable to

nitrate ligands, and the latter exhibits a relatively weaker complexing ability compared with other acid ligands and a weaker field compared with water molecules.

Since all adsorbed metal ions correspond to the  $3d^n4s^0$  electronic structure (configuration), they are potentially capable of forming aqua ions in aqueous solutions in the form of highly symmetrical inner-sphere octahedral complexes with a coordination number of 6. The aqua ligand has a relatively weak field, so, octahedral complexes with either  $d^2sp^3$  or  $sp^3d^2$  hybridization can be formed.

All studied metal ions have unpaired electrons in the 3d orbital. However,  $\text{Cr}^{3+}$  ions, unlike other ions have two free orbitals at the 3d sublevel, which provides strong bonds when an octahedral complex with  $d^2sp^3$  hybridization of electron orbitals is formed. This type of hybridization unlike the outer-sphere  $sp^3d^2$  hybridization makes it possible to obtain a stabler complex. The smaller radius and the stabler inner-sphere complex promote the higher polarization of the aqua ligand, which allows  $\text{Cr}^{3+}$  ions to exhibit a greater tendency to hydrolysis.

The difference in the behavior of metal ions is essentially related to the Jahn–Teller effect [49]. The high symmetry (the octahedral configuration of the inner-sphere complex) is due to the degeneracy of the electronic states of the central metal ion. However, in the case of unpaired electrons in the electronic structure, such configuration containing degenerate states of electrons is unstable. Due to the Jahn–Teller effect the inner-sphere octahedral complexes of metal ions can be distorted. This distortion is most pronounced for  $\text{Cu}^{2+}$  ions. The distortion is so considerable that a decrease in symmetry leads to transformation of the octahedral coordination into tetrahedral one with a decrease in the coordination number of the inner-sphere complex. As a result, the degree of hydration of the ion may decrease.

So, the sorption of metal ions on titanium phosphate is a complex effect of various interactions, resulting in the formation of chelate bonds between the metal ion and ionogenic phosphate groups. The formation of chelate bonds leads to an increase in the stability of the electronic state of metal ions that in turn promote decrease in the symmetry of their nearest environment. The reason for this energetically more favorable state is both entropy and enthalpy factors. The entropy

factor plays a the main role in sorption process. The replacement of lithium ions by guest ions, dehydration of the latter and their interaction with phosphate groups lead to increase in the total number of free ions and molecules in the system, which in turn, causes an increase in entropy. However, the enthalpy effect is also important. This effect is associated with decrease in the length of the chelate bond of the guest ions with phosphate groups. The formation of chemical bonds that are much stronger than ordinary ones releases energy from the system and facilitates the sorption process.

The experimental results on the sorption of metal ions in saturated LiNO<sub>3</sub> solution on Li-TiOP demonstrate the important factors, influencing the equilibrium of sorption process to be the size of the solvated metal ion, its effective charge, the electronic structure of the sorbed ion, and their interaction with the functional groups of the sorbent.

### 3.4 Sorption ability of Li-TiOP in multi-component system

The first model solution was prepared having the concentration of each metal cation of 0.2 mmol/L, and the concentration of metal ions in

the second solution was 0.1 mmol/L. To assess the purification efficiency, the required standards of Li solution for producing optical materials are given in Table 6.

**Table 6** Limits of impurity content in Li solution

Element	Content/wt.%	Concentration/(g·L <sup>-1</sup> )
Mn	0.00005	≤1.72×10 <sup>-4</sup>
Co	0.00002	≤6.89×10 <sup>-5</sup>
Ni	0.00002	≤6.89×10 <sup>-5</sup>
Cu	0.00005	≤1.72×10 <sup>-4</sup>
Cr	0.00005	≤1.72×10 <sup>-4</sup>

Sorption efficiency  $S_{\text{eff}}$  towards Cu<sup>2+</sup> and Cr<sup>3+</sup> ions is found to be 99.6%–99.9% at the first stage (Table 7), and the residual concentration of metal ions in the solution is lower than the required standard of impurities. To remove Mn<sup>2+</sup>, Co<sup>2+</sup> and Ni<sup>2+</sup> ions, additional purification stage is needed for the chosen concentration of impurities. For the final treatment of lithium solution (second stage) the spent sorbent is separated by filtration, and fresh portion of Li-TiOP is loaded into filtrate.

The results show that  $K_d$  values for Cu<sup>2+</sup> and Cr<sup>3+</sup> ions noticeably exceed those of Mn<sup>2+</sup>, Co<sup>2+</sup>,

**Table 7** Adsorption data for sorption of impurities on Li-TiOP from complex solutions

Stage	Parameter	Mn <sup>2+</sup>	Co <sup>2+</sup>	Ni <sup>2+</sup>	Cu <sup>2+</sup>	Cr <sup>3+</sup>
1st	$C_o/(g \cdot L^{-1})$	0.0110	0.0118	0.0117	0.0127	0.0104
	$C_e^{(1)}/(g \cdot L^{-1})$	$4.07 \times 10^{-4}$	$5.89 \times 10^{-4}$	$7.34 \times 10^{-4}$	$5.24 \times 10^{-5}$	$5.20 \times 10^{-5}$
	$S_{\text{eff}}/\%$	96.3	95.0	93.7	99.6	99.9
	$K_d/(cm^3 \cdot g^{-1})$	$3.0 \times 10^3$	$3.8 \times 10^3$	$2.9 \times 10^3$	$4.8 \times 10^4$	$4.0 \times 10^4$
2nd	$C_e^{(1)}/(g \cdot L^{-1})$	$4.07 \times 10^{-4}$	$5.89 \times 10^{-4}$	$7.34 \times 10^{-4}$	–	–
	$C_e^{(2)}/(g \cdot L^{-1})$	$1.51 \times 10^{-5}$	$2.95 \times 10^{-5}$	$4.59 \times 10^{-5}$	–	–
	$S_{\text{eff}}/\%$	96.3	95.0	93.7	–	–
	$K_d/(cm^3 \cdot g^{-1})$	$5.1 \times 10^3$	$3.7 \times 10^3$	$3.0 \times 10^3$	–	–
1st	$C_o/(g \cdot L^{-1})$	0.00549	0.00589	0.00587	0.00635	0.0052
	$C_e^{(1)}/(g \cdot L^{-1})$	$2.03 \times 10^{-4}$	$2.94 \times 10^{-4}$	$3.67 \times 10^{-4}$	$1.32 \times 10^{-5}$	$1.29 \times 10^{-5}$
	$S_{\text{eff}}/\%$	96.3	95	93.7	99.8	99.7
	$K_d/(cm^3 \cdot g^{-1})$	$5.2 \times 10^3$	$3.8 \times 10^3$	$3.0 \times 10^3$	$9.6 \times 10^4$	$8.0 \times 10^4$
2nd	$C_o/(g \cdot L^{-1})$	$2.03 \times 10^{-4}$	$2.94 \times 10^{-4}$	$3.67 \times 10^{-4}$	–	–
	$C_e^{(1)}/(g \cdot L^{-1})$	$2.50 \times 10^{-5}$	$3.89 \times 10^{-5}$	$5.58 \times 10^{-5}$	–	–
	$S_{\text{eff}}/\%$	87.6	86.8	84.8	–	–
	$K_d/(cm^3 \cdot g^{-1})$	$1.4 \times 10^3$	$1.3 \times 10^3$	$1.1 \times 10^3$	–	–

$V:m=200$  L/g;  $K_d$  is distribution coefficient of ions

and  $\text{Ni}^{2+}$ , which correlates well with the sorption constants from the results of the sorption equilibrium study. The values of  $K_d$  are found to be ( $\text{cm}^3/\text{g}$ ):  $\text{Mn}^{2+}$   $(1.4\text{--}5.2)\times 10^3$ ,  $\text{Co}^{2+}$   $(1.3\text{--}3.8)\times 10^3$ ,  $\text{Ni}^{2+}$   $(1.1\text{--}3.0)\times 10^3$ ,  $\text{Cu}^{2+}$   $(4.8\text{--}9.6)\times 10^4$  and  $\text{Cr}^{3+}$   $(4.0\text{--}8.0)\times 10^4$ . High  $K_d$  values determine the possibility of the effective removal of trace concentrations of heavy metals on the lithium substituted titanium phosphate from complex solutions, resulting in  $\text{LiNO}_3$  purity level of  $>99.999$  wt.%.

The analysis of the Langmuir isotherm parameters confirms the above conclusion. So, according to WEBER and CHAKRAVORTI [50], the dimensionless separation factor ( $R_L$ ) was calculated as follows:

$$R_L = \frac{1}{1 + bC_0} \quad (18)$$

where  $C_0$  is the initial sorbate concentration.

The  $R_L$  values are estimated to be 0.002, 0.018, 0.03, 0.047 and 0.125 for  $\text{Cr}^{3+}$ ,  $\text{Cu}^{2+}$ ,  $\text{Mn}^{2+}$ ,  $\text{Co}^{2+}$  and  $\text{Ni}^{2+}$ , respectively. A lower  $R_L$  value indicates the more efficient adsorption. Obviously, the sorption process is completely appreciable for all the ions. The results show that the selectivity of Li-TiOP towards the metal ions in the complex solution decreases in the following order:  $\text{Cr}^{3+} > \text{Cu}^{2+} > \text{Mn}^{2+} > \text{Co}^{2+} > \text{Ni}^{2+}$ . Thus, the comparison of the sorption constants and distribution coefficients of ions indicates the possibility of the purification of saturated  $\text{LiNO}_3$  multi-component solutions up to the level of required standard.

## 4 Conclusions

(1) The sorption of impurities ( $\text{Mn}^{2+}$ ,  $\text{Co}^{2+}$ ,  $\text{Cu}^{2+}$ ,  $\text{Ni}^{2+}$  and  $\text{Cr}^{3+}$ ) on amorphous Li-TiOP in saturated  $\text{LiNO}_3$  solution was investigated. The adsorption isotherms for studied metal ions on the Li-TiOP sorbent were considered using the Langmuir, Freundlich, Temkin and Nikolsky models. Among the four models, the Langmuir and Nikolsky simulations are found to be consistent with experimental data ( $R^2=0.997\text{--}0.999$ ).

(2) The cation selectivity order for Li-TiOP determined by experiments is established to be  $\text{Cr}^{3+} > \text{Cu}^{2+} > \text{Mn}^{2+} > \text{Co}^{2+} > \text{Ni}^{2+}$  for all selected models. The difference in sorption efficiency is attributed to the size of the hydration shell of sorbed

ions.

(3) Thermodynamic parameters of the sorption process are calculated, and it was found that the change in the entropy and enthalpy of the sorption process is correlated with that in the ionic potential of the sorbent.

(4) Also, it has been demonstrated that the electronic structure of the sorbed ion affects its sorption ability.

(5) We have successfully purify the concentrated  $\text{LiNO}_3$  solution containing transition metal impurities by sorption on Li-TiOP to obtain a high purity grade lithium nitrate of  $>99.999$  wt.%. Cu and Cr ions were removed in a single sorption step with residual concentration of impurities less than  $5.3\times 10^{-5}$  g/L. The second sorption step enables the removal of Co, Ni and Mn ions with the residual concentration of impurities below the required standard.

## References

- [1] SWAIN B. Recovery and recycling of lithium: A review [J]. Separation and Purification Technology, 2017, 172: 388–403.
- [2] LEI Shu-ya, CAO Yang, CAO Xue-feng, SUN Wei, WENG Ya-qing, YANG Yue. Separation of lithium and transition metals from leachate of spent lithium-ion batteries by solvent extraction method with Versatic 10 [J]. Separation and Purification Technology, 2020, 250: 117258.
- [3] DESSEMOND C, LAJOIE-LEROUX F, SOUCY G, LAROCHE N, MAGNAN J F. Spodumene: The lithium market, resources and processes [J]. Minerals, 2019, 9(6): 334.
- [4] KUMAR A, CHAKRABARTI A, SHEKHAWAT M S, MOLLA A R. Transparent ultra-low expansion lithium aluminosilicate glass-ceramics: Crystallization kinetics, structural and optical properties [J]. Thermochemica Acta, 2019, 676: 155–163.
- [5] DESHPANDE V K, JAGDALE M V. Effect of  $\text{Li}_2\text{O}\text{--}\text{B}_2\text{O}_3\text{--}\text{SiO}_2\text{--}\text{Nb}_2\text{O}_5$  glass addition on dielectric and ferroelectric properties of lithium niobate ceramics [J]. Ferroelectrics, 2017, 510(1): 95–102.
- [6] LI G R, YIN Q R, ZHENG L Y, GUO Y Y, CAO W W. Dielectric and piezoelectric properties of sodium lithium niobate  $\text{Na}_{1-x}\text{Li}_x\text{NbO}_3$  lead free ferroelectric ceramics [J]. Journal of Electroceramics, 2008, 21(1/2/3/4): 323–326.
- [7] ŠMIGA W, GARBARZ-GLOS B, LIVINSH M, SMELTERE I. Influence of lithium substitution on structure, electric and pyroelectric properties of sodium niobate ceramics [J]. Ferroelectrics, 2012, 436(1): 54–61.
- [8] GABRA G G, TORMA A E, OLIVIER C A. Pressure leaching of beta-spodumene by sodium chloride [J]. Canadian Metallurgical Quarterly, 1975, 14(4): 355–359.
- [9] van LUONG T, KANG D J, AN J W, KIM M J, TRAN T.

- Factors affecting the extraction of lithium from lepidolite [J]. *Hydrometallurgy*, 2013, 134/135: 54–61.
- [10] KUANG Ge, LIU Yu, LI Huan, XING Sheng-zhou, LI Fu-jie, GUO Hui. Extraction of lithium from  $\beta$ -spodumene using sodium sulfate solution [J]. *Hydrometallurgy*, 2018, 177: 49–56.
- [11] MENG Fei, MCNEICE J, ZADEH S S, GHAREMAN A. Review of lithium production and recovery from minerals, brines, and lithium-ion batteries [J]. *Mineral Processing and Extractive Metallurgy Review*, 2021, 42(2): 123–141.
- [12] XU Wen-hua, LIU Dong-fu, HE Li-hua, ZHAO Zhong-wei. A comprehensive membrane process for preparing lithium carbonate from high Mg/Li brine [J]. *Membranes*, 2020, 10(12): 371.
- [13] HAMZAOU A H, M'NIF A, HAMMI H, ROKBANI R. Contribution to the lithium recovery from brine [J]. *Desalination*, 2003, 158(1/2/3): 221–224.
- [14] JIANG Chen-xiao, WANG Yao-ming, WANG Qiu-yue, FENG Hong-yan, XU Tong-wen. Production of lithium hydroxide from lake brines through electro-electrodialysis with bipolar membranes (EEDBM) [J]. *Industrial & Engineering Chemistry Research*, 2014, 53(14): 6103–6112.
- [15] LIU Xu-heng, CHEN Xing-yu, HE Li-hua, ZHAO Zhong-wei. Study on extraction of lithium from salt lake brine by membrane electrolysis [J]. *Desalination*, 2015, 376: 35–40.
- [16] PELLY I. Recovery of lithium from Dead Sea brines [J]. *Journal of Applied Chemistry and Biotechnology*, 1978, 28(7): 469–474.
- [17] EPSTEIN J A, FEIST E M, ZMORA J, MARCUS Y. Extraction of lithium from the Dead Sea [J]. *Hydrometallurgy*, 1981, 6(3/4): 269–275.
- [18] LINNEEN N, BHAVE R, WOERNER D. Purification of industrial grade lithium chloride for the recovery of high purity battery grade lithium carbonate [J]. *Separation and Purification Technology*, 2019, 214: 168–173.
- [19] LIU Wei, CHU Guang-wen, LI Shao-chen, BAI Shun, LUO Yong, SUN Bao-chang, CHEN Jian-feng. Preparation of lithium carbonate by thermal decomposition in a rotating packed bed reactor [J]. *Chemical Engineering Journal*, 2019, 377: 119929.
- [20] WANG Wei, CHEN Wei-jie, LIU Hai-tao. Hydro-metallurgical preparation of lithium carbonate from lithium-rich electrolyte [J]. *Hydrometallurgy*, 2019, 185: 88–92.
- [21] UM N, HIRATO T. Precipitation behavior of  $\text{Ca}(\text{OH})_2$ ,  $\text{Mg}(\text{OH})_2$ , and  $\text{Mn}(\text{OH})_2$  from  $\text{CaCl}_2$ ,  $\text{MgCl}_2$ , and  $\text{MnCl}_2$  in  $\text{NaOH-H}_2\text{O}$  solutions and study of lithium recovery from seawater via two-stage precipitation process [J]. *Hydrometallurgy*, 2014, 146: 142–148.
- [22] GAO Ao-lei, SUN Zhen-hua, LI Shao-peng, HOU Xin-juan, LI Hui-quan, WU Qi-sheng, XI Xin-guo. The mechanism of manganese dissolution on  $\text{Li}_{1.6}\text{Mn}_{1.6}\text{O}_4$  ion sieves with HCl [J]. *Dalton Transactions*, 2018, 47(11): 3864–3871.
- [23] YANG Fan, CHEN Si-chong, SHI Chen-tao, XUE Feng, ZHANG Xiao-xian, JU Shen-gui, XING Wei-hong. A facile synthesis of hexagonal spinel  $\lambda$ - $\text{MnO}_2$  ion-sieves for highly selective  $\text{Li}^+$  adsorption [J]. *Processes*, 2018, 6(5): 59.
- [24] HUI Zhong. Property of  $\text{H}_2\text{TiO}_3$  type ion-exchangers and extraction of lithium from brine of natural gas wells [J]. *Chinese Journal Applied Chemistry*, 2000, 17: 307–309.
- [25] CHITRAKAR R, MAKITA Y, OOI K, SONODA A. Lithium recovery from salt lake brine by  $\text{H}_2\text{TiO}_3$  [J]. *Dalton Transactions*, 2014, 43(23): 8933–8939.
- [26] KINUGASA T, NISHIBARA H, MURAO Y, KAWAMURA Y, WATANABE K, TAKEUCHI H. Equilibrium and kinetics of lithium extraction by a mixture of LIX54 and TOPO [J]. *Journal of Chemical Engineering of Japan*, 1994, 27(6): 815–818.
- [27] SHI Cheng-long, JING Yan, XIAO Jiang, WANG Xing-quan, YAO Ying, JIA Yong-zhong. Solvent extraction of lithium from aqueous solution using non-fluorinated functionalized ionic liquids as extraction agents [J]. *Separation and Purification Technology*, 2017, 172: 473–479.
- [28] ZHOU Zhi-yong, QIN Wei, FEI Wei-yang. Extraction equilibria of lithium with tributyl phosphate in three diluents [J]. *Journal of Chemical & Engineering Data*, 2011, 56(9): 3518–3522.
- [29] GAO Dao-lin, YU Xiao-ping, GUO Ya-fei, WANG Shi-qiang, LIU Ming-ming, DENG Tian-long, CHEN Yu-wei, BELZILE N. Extraction of lithium from salt lake brine with triisobutyl phosphate in ionic liquid and kerosene [J]. *Chemical Research in Chinese Universities*, 2015, 31(4): 621–626.
- [30] GAO Dao-lin, GUO Ya-fei, YU Xiao-ping, WANG Shi-qiang, DENG Tian-long. Extracting lithium from the high concentration ratio of magnesium and lithium brine using imidazolium-based ionic liquids with varying alkyl chain lengths [J]. *Journal of Chemical Engineering of Japan*, 2016, 49(2): 104–110.
- [31] SUN Shu-ying, CAI Li-juan, NIE Xiao-yao, SONG Xing-fu, YU Jian-guo. Separation of magnesium and lithium from brine using a Desal nanofiltration membrane [J]. *Journal of Water Process Engineering*, 2015, 7: 210–217.
- [32] MILYUTIN V V, NEKRASOVA N A, RUDSKIKH V V, VOLKOVA T S. Preparation of high-purity lithium carbonate using complexing ion-exchange resins [J]. *Russian Journal of Applied Chemistry*, 2020, 93(4): 549–553.
- [33] PATTERSON W M, STARK P C, YOSHIDA T M, SHEIK-BAHAE M, HEHLEN M P. Preparation and characterization of high-purity metal fluorides for photonic applications [J]. *Journal of the American Ceramic Society*, 2011, 94(9): 2896–2901.
- [34] HEHLEN M P, BONCHER W L, MELGAARD S D, BLAIR M W, JACKSON R A, LITTLEFORD T E, LOVE S P. Preparation of high-purity  $\text{LiF}$ ,  $\text{YF}_3$ , and  $\text{YbF}_3$  for laser refrigeration [C]/*Proceedings of SPIE. California, UAS*: 2014: 14–24.
- [35] JIA Kun, PAN Bing-cai, ZHANG Qing-rui, ZHANG Wei-ming, JIANG Pei-juan, HONG Chang-hong, PAN Bing-jun, ZHANG Quan-xing. Adsorption of  $\text{Pb}^{2+}$ ,  $\text{Zn}^{2+}$ , and  $\text{Cd}^{2+}$  from waters by amorphous titanium phosphate [J]. *Journal of Colloid and Interface Science*, 2008, 318(2): 160–166.
- [36] BORBA C E, SILVA E A, SPOHR S, SANTOS G H F, GUIRARDELLO R. Application of the mass action law to describe ion exchange equilibrium in a fixed-bed column [J]. *Chemical Engineering Journal*, 2011, 172: 312–320.

- [37] MASLOVA M, MUDRUK N, IVANENKO V, GERASIMOVA L. Highly efficient synthesis of titanium phosphate precursor for electroactive materials [J]. *Ceramics International*, 2022, 48: 2257–2272.
- [38] HANAOR D A H, SORRELL C C. Review of the anatase to rutile phase transformation [J]. *Journal of Materials Science*, 2011, 46(4): 855–874.
- [39] TRUBLET M, MASLOVA M V., RUSANOVA D, ANTZUTKIN O N. Sorption performances of  $\text{TiO}(\text{OH})(\text{H}_2\text{PO}_4)\cdot\text{H}_2\text{O}$  in synthetic and mine waters [J]. *RSC Advances*, 2017, 7(4): 1989–2001.
- [40] MASLOVA M, IVANENKO V, YANICHEVA N, GERASIMOVA L. The effect of heavy metal ions hydration on their sorption by a mesoporous titanium phosphate ion-exchanger [J]. *Journal of Water Process Engineering*, 2020, 35: 101233.
- [41] CLEARFIELD A, BORTUN A I, KHAINAKOV S A, BORTUN L N, STRELKO V V, KHRYASCHEVSKII V N. Spherically granulated titanium phosphate as exchanger for toxic heavy metals [J]. *Waste Management*, 1998, 18(3): 203–210.
- [42] ROCA S, AIROLDI C. Thermodynamic data of ion exchange on amorphous titanium(IV) phosphate [J]. *Thermochimica Acta*, 1996, 284(2): 289–297.
- [43] GREVILLOT G, DZYAZKO J, KAZDOBIN K A, BELYAKOV V. The electrochemically controlled sorption of d-metal cations by ion exchangers based on titanium phosphate [J]. *Journal of Solid State Electrochemistry*, 1999, 3(2): 111–116.
- [44] NUNES L M, PARENTE B, MAURERA M A M, AIROLDI C. Cobalt, nickel, and copper ion-exchanged on heterocyclic amine-intercalated titanium hydrogenphosphate compounds [J]. *Industrial & Engineering Chemistry Research*, 2008, 47(15): 5441–5446.
- [45] YU Kai, AI Zheng-rong, NING Zhi-qiang, HU Wei, XIE Hong-wei. Adsorption process in aqueous solution of silver nitrate by ion exchange method [J]. *Chinese Journal of Rare Metals*, 2021, 45(11):1352–1358.
- [46] HAYNES W M. CRC handbook of chemistry and physics [M]. Boca Raton: Taylor & Francis Group, 2016.
- [47] SAHU B B, PARIDA K. Cation exchange and sorption properties of crystalline  $\alpha$ -titanium(IV) phosphate [J]. *Journal of Colloid and Interface Science*, 2002, 248(2): 221–230.
- [48] BOKII G B. Crystallochemistry [M]. Khimiya, Moscow, 1971: 400.
- [49] PEARSON R G. Concerning Jahn–Teller effects [J]. *Proceedings of the National Academy of Sciences of the United States of America*, 1975, 72(6): 2104–2106.
- [50] WEBER T W, CHAKRAVORTI R K. Pore and solid diffusion models for fixed-bed adsorbers [J]. *AIChE Journal*, 1974, 20(2): 228–238.

## 磷酸钛离子交换剂纯化饱和 $\text{LiNO}_3$ 溶液的平衡

V. I. IVANENKO, M. V. MASLOVA, P. E. EVSTROPOVA, L. G. GERASIMOVA

Tananaev Institute of Chemistry and Technology of Federal Research Centre,  
Kola Science Centre of the Russian Academy of Sciences, Apatity, Russia

**摘要:** 研究磷酸钛离子交换剂(Li-TiOP)在饱和  $\text{LiNO}_3$  溶液中对  $\text{Cu}^{2+}$ 、 $\text{Co}^{2+}$ 、 $\text{Mn}^{2+}$ 、 $\text{Ni}^{2+}$ 和  $\text{Cr}^{3+}$ 离子的吸附性能。采用 XRD、SEM、TG、DSC、NGSP 和元素分析对固体样品进行表征。采用原子吸收光谱法(AAS)和电感耦合等离子体质谱法(ICP MS)测定溶液中离子的浓度。采用 Langmuir、Freundlich、Temkin 和 Nikolsky 模型计算金属离子的吸附等温线。在研究金属离子吸附时, 必须考虑吸附剂的溶剂化状态。Li-TiOP 对所研究离子的选择性为:  $\text{Cr}^{3+} > \text{Cu}^{2+} > \text{Mn}^{2+} > \text{Co}^{2+} > \text{Ni}^{2+}$ , 且对上述 4 种模型均适用。吸附过程热力学参数的变化与吸附剂离子电位的变化有关。磷酸钛能有效去除多组分溶液中的微量金属离子, 使  $\text{LiNO}_3$  纯度高于 99.999%(质量分数)。

**关键词:** 硝酸锂; 磷酸钛; 提纯; 过渡金属元素; 吸附; 吸附等温线; 热力学

(Edited by Xiang-qun LI)